Second Messengers Regulate Endosomal Acidification in Swiss 3T3 Fibroblasts

Ke Zen, Joachim Biwersi, N. Periasamy, and A. S. Verkman

Departments of Medicine and Physiology, Cardiovascular Research Institute and Cystic Fibrosis Research Center, University of California, San Francisco, California 94143

Abstract. Acidification of the endosomal pathway is important for ligand and receptor sorting, toxin activation, and protein degradation by lysosomal acid hydrolases. Fluorescent probes and imaging methods were developed to measure pH to better than 0.2 U accuracy in individual endocytic vesicles in Swiss 3T3 fibroblasts. Endosomes were pulse labeled with transferrin (Tf), α_2-macroglobulin (α_2M), or dextran, each conjugated with tetramethylrhodamine and carboxyfluorescein (for pH 5–8) or dichlorocarboxyfluorescein (for pH 4–6); pH in individual labeled vesicles was measured by ratio imaging using a cooled CCD camera and novel image analysis software. Tf-labeled endosomes acidified to pH 6.2 ± 0.1 with a $t_{1/2}$ of 4 min at 37°C, and remained small and near the cell periphery. Dextran- and α_2M-labeled endosomes acidified to pH 4.7 ± 0.2, becoming larger and moving toward the nucleus over 30 min; ~15% of α_2M-labeled endosomes were strongly acidic (pH < 5.5) at only 1 min after labeling. Replacement of external Cl by NO_3 or isethionate strongly and reversibly inhibited acidification. Addition of ouabain (1 mM) at the time of labeling strongly enhanced acidification in the first 5 min; Tf-labeled endosomes acidified to pH 5.3 without a change in morphology. Activation of phospholipase C by vasopressin (50 nM) enhanced acidification of early endosomes; activation of protein kinase C by PMA (100 nM) enhanced acidification strongly, whereas elevation of intracellular Ca by A23187 (1 μM) had no effect on acidification. Activation of protein kinase A by CPT-cAMP (0.5 mM) or forskolin (50 μM) inhibited acidification. Lysosomal pH was not affected by ouabain or the protein kinase activators. These results establish a methodology for quantitative measurement of pH in individual endocytic vesicles, and demonstrate that acidification of endosomes labeled with Tf and α_2M (receptor-mediated endocytosis) and dextran (fluid-phase endocytosis) is sensitive to intracellular anion composition, Na/K pump inhibition, and multiple intracellular second messengers.

THE acidification of organelles in the endocytic pathway plays an important role in the intracellular trafficking and biochemical processing of internalized receptors, bound ligands, and fluid-phase solutes (for review see Mellman et al., 1986). There is considerable variation in the pH of endocytic compartments. The pH of endocytic vesicles routed to lysosomes decreases progressively, from 6–6.5 for "early" endosomes, to 5.5–6 for "sorting" endosomes or "multi-vesicular bodies", to 4.5–5.5 for "late" endosomes and lysosomes. Selected ligands, such as transferrin, pass through mildly acidic (pH 6–6.5) "recycling" endosomes without transport to lysosomes (Sipe and Murphy, 1987; Yamashiro and Maxfield, 1987), whereas others, such as α_2-macroglobulin, are transported to lysosomes (Yamashiro and Maxfield, 1984). As a unique example, the vasopressin-regulated water channel in epithelial cells from kidney and amphibian urinary bladder was found to remain in a non-acidic compartment (pH >7.2) after endocytic retrieval from the apical membrane (Lencer et al., 1990; Wang et al., 1991). It has been proposed recently that defective acidification of organelles in the endocytic and secretory pathways has a central role in the pathophysiology of the genetic disease cystic fibrosis (Barasch et al., 1991), where a variety of phenotypic defects at the cellular level have been associated with the cystic fibrosis genotype.

Several factors can in principle control the pH of endocytic vesicles. The number and activity of vacuolar-type proton ATPases in the endosomal membrane would provide a first level of control. Because proton ATPase action is electrogenic, inward proton pumping must be accompanied by parallel inward anion (Cl) movement, and/or outward cation (Na or K) movement. Therefore the activity of endosomal ion conductances could regulate pH. Further, because the activity of the proton ATPase depends upon the proton electrochemical potential, pH can be controlled by factors that set membrane potential, such as the activity of other electrogenic ion pumps. Endosomal pH can also be controlled by the rate at which the pH gradient between endosomal and cy-

toplasmic compartments is dissipated by passive proton efflux, which depends upon the membrane proton conductance ("proton leak") and/or ion-coupled proton transporters. Finally, the ion and proton electrochemical gradients depend on cytoplasmic ion activities and pH. The regulation of any of these factors by intracellular ion composition or second messengers could influence endosomal pH and thus have profound effects on endosomal trafficking.

Although a large body of information exists on the morphology and kinetics of the endocytic pathway, relatively little is known about whether and how endosomal acidification is regulated in living cells. In cell-free experiments performed on endosomes and lysosomes isolated from different cell types (for review see Gruenberg and Howell, 1989; Van Dyke, 1990), there is evidence that ATP-dependent acidification by the proton ATPase may be controlled, in part, by passive conductances to Cl (Van Dyke, 1988; Barasch et al., 1988; Blair et al., 1991), cations (Lukacs et al., 1991), and protons (Fuchs et al., 1989*a*), and an ATP-dependent Na/K pump (Fuchs et al., 1989*b*). In isolated endocytic vesicles from kidney proximal tubule (Bae and Verkman, 1990; Reenstra et al., 1992) and liposomes reconstituted with proteins from clathrin-coated vesicles (Mulberg et al., 1991), a protein kinase A–activated Cl channel has been identified. It was proposed that activation of the Cl channel might facilitate endosomal acidification by providing a shunt to dissipate the interior-positive potential produced by the proton pump. In suspended A549 cells labeled with FITC-transferrin, inhibition of the Na/K ATPase pump by ouabain enhanced acidification (Cain et al., 1989), suggesting that the interior-positive potential produced by internalized Na/K pumps (one cycle pumps 3 Na inward and 2 K outward) regulates acidification of early endosomes. In endosomes containing the vasopressin-inducible water channel, the lack of measurable acidification has been ascribed to the absence of selected subunits of the vacuolar-type proton pump (Sabolic et al., 1992). Taken together, these findings suggest that acidification of the endocytic pathway in some cell types may be subject to physiological regulation.

The goal of this study was to determine whether acidification of endosomes in intact Swiss 3T3 fibroblasts is regulated by second messengers, intracellular ion composition, and an Na/K ATPase. The experimental approach was to pulse label endosomes with dual-wavelength fluorescent indicators of receptor-mediated and fluid-phase endocytosis. The indicators that were synthesized include transferrin, α_2-macroglobulin and dextran, each conjugated with pH-sensitive (carboxyfluorescein or dichlorocarboxyfluorescein) and pH-insensitive (tetramethylrhodamine) chromophores. At specified times after labeling, pH in a series of individual endocytic vesicles in a single microscope field was determined quantitatively by ratio imaging using a cooled CCD camera. Possible regulators of acidification could be added at any time before, during, or after the pulse labeling. It was found that acidification of "early" endosomes was strongly enhanced by ouabain and protein kinase C activation, and inhibited by protein kinase A activation, and that endosomal acidification was sensitive to intracellular ion composition. The experiments also provided direct information about the time course of the distribution of pH values as a cohort of labeled endocytic vesicles undergoes intracellular trafficking.

Materials and Methods

Materials

Aminodextran (mol wt 40,000), 5(and 6)-carboxy-2',6'-dichlorofluorescein (Cl_2CF),[1] 5(and 6)-carboxyfluorescein (CF) succinimidylester, and 5(and 6)-carboxytetramethylrhodamine (TMR) succinimidylester were obtained from Molecular Probes, Inc. (Eugene, OR), human transferrin (Tf) from Sigma Chemical Co. (St. Louis, MO), bovine α_2-macroglobulin (α_2M) from Boehringer Mannheim (Indianapolis, IN). All other chemicals were purchased from Aldrich Chemical Co. (Milwaukee, WI).

Synthesis of the Fluorescent Ligands

Cl_2-CF succinimidylester: 0.1 mmol *N*-hydroxysuccinimide and 0.2 mmol trifluoroacetanhydride (TFA) were stirred at 20°C for 30 min. After vacuum evaporation of the excess TFA, 0.067 mmol Cl_2 CF in 2ml THF was added and the mixture was stirred for 24 h. The THF was evaporated and the residue was washed with ether and filtered.

Fluorescent labeling of aminodextran, Tf and α_2M: 20 mg (aminodextran, Tf, or α_2M), 3.5 mg (CF-succinimidylester or Cl_2CF-succinimidylester), and 1.1 mg TMR-succinimidylester were dissolved in 5 ml 50 mM aqueous Na borate (pH, 9) and stirred for 3 h at 20°C, and then 21 h at 4°C. The reaction product was dialyzed with 0.5 mM Na phosphate buffer (pH, 7.4) for >36 h and lyophilized. Thin layer chromatography showed absence of unconjugated dyes. Using molar absorbance data, dye-to-(dextran/protein) molar labeling ratios were 1.5–2.5 mol (CF or Cl_2CF), and 0.5–0.7 mol TMR per 10,000 mol wt dextran/protein.

Cell Culture and Labeling

Swiss 3T3 fibroblasts (No. CL-101; American Type Collection, Rockville, MD) were grown on 18-mm-diam round glass coverslips in DME-H21 supplemented with 5% bovine calf serum, 100 U/ml penicillin, and 100 g/ml streptomycin. Cells were maintained at 37°C in a 95% air/5% CO_2 incubator and used 2–4 d after plating. Coverslips were transferred to a 200-μL perfusion chamber in which the cell-free surface of the coverglass made contact with the immersion objective (Chao et al., 1989). Cells were perfused continuously with a physiological buffer (buffer A: 138 mM NaCl, 2.7 mM KCl, 0.7 mM $CaCl_2$, 1.1 mM $MgCl_2$, 1.5 mM KH_2PO_4, 8.1 mM Na_2HPO_4, 5 mM glucose, pH 7.4) at 37°C. In some studies, Cl was replaced by NO_3 (buffer B) or isethionate (buffer C). Endocytic vesicles were pulse labeled with fluorescent indicators (Tf or α_2M, 100–150 μg/ml; dextrans, 5 mg/ml) for 30 s in the perfusion chamber. After labeling (defined as 0 time), cells were perfused continuously with appropriate buffer. Perfusates could be changed at specified times by a four way valve (Hamilton Co., Reno, NV). In some experiments, cells were perfused for 5–10 min with the non-fluorescent buffer at 10°C just after labeling to remove better the extracellular dye. The low temperature washing step did not affect subsequent endosome pH measurements performed at 37°C.

Microscopy Measurements

Experiments were carried out on an epifluorescence microscope (Leitz, Rochleigh, NJ) equipped with a coaxial-confocal attachment (Technical Instruments, San Francisco, CA). Cells were viewed with a 60× oil immersion objective with a numerical aperture of 1.4 (Plan-Apo objective, working distance 0.17 mm; Nikon Inc., Garden City, NY). The light source was a stabilized Hg-Xe arc lamp (100 W) equipped with an iris diaphragm, electronic shutter (Uniblitz, model D122 controller; Vincent Associates, Rochester, NJ) and standard FITC and rhodamine filter sets. Fluorescence images were obtained by a cooled charged coupled device (CCD) camera (AT200 series; Photometrics, Tucson, AZ) with type TK512CB detector (Tektronix, Inc., Beaverton, OR). An electronic shutter was positioned between the sample and detector. The detector consisted of 512 × 512 pixels with a dynamic range of 16,384 gray levels (14 bits); the quantum efficiency was >0.85 in the wavelength range 400–800 nm, and the dark noise was 2.6 electrons/s per pixel at −40°C. The pixel response linearity and gain

1. *Abbreviations used in this paper*: α_2M, α_2-macroglobulin; CCD, charged coupled device; CF, carboxyfluorescein; Cl_2CF, dichlorocarboxyfluorescein; CPT, chlorophenylthio; Tf, transferrin; TMR, carboxytetramethylrhodamine.

were examined by recording a series of images of a uniformly illuminated target for five equally spaced acquisition times in the range 1–12 s; the gain and zero offset of each pixel was determined by a linear regression of pixel intensity to acquisition time. The response of each pixel (excluding border pixels) to light was linear ($r > 0.998$) and pixel gains were uniform with an SD of 3.2% of mean gain; <0.06% of pixels had gains outside of 3 SD. The control of image acquisition, including timing, shutter control, filter selection, size definition, data read out and storage, was programmed on a dedicated 486 CPU computer using custom-written software in C language with some functions provided in the Photometrics software library.

The sequence of operations in a typical experiment involving acquisition of image pairs (rhodamine and FITC, 1–2 s acquisition, 100 ms between images) at different times after pulse labeling of cells ($t = 0$) were as follows: After a visual check of the cells, the image was focused, and image size (typically 300 × 200 pixels) was selected. A pair of "dark" images (which includes pixel bias values) for subtraction were obtained with excitation shutter closed. Pairs of fluorescence images for the two filter sets were then acquired at software programmable times. The corrected images were stored on a 160 Mb hard disk for subsequent analysis. Excitation and emission shutters were closed between acquisitions, although if desired, images could be examined and refocused at any time. At the end of a measurement set, cells were perfused with buffered solutions at low (pH 4) and high pH (pH 8) containing high K (100 mM Na replaced by K) and 5 μM nigericin for internal calibration and sets of image pairs were obtained. After filling 100 Mb of memory, images were archived on a 2 Gbyte digital tape using a CY8200 tape drive (Cybernetics Group, Newport News, VA).

Image Analysis Routines

The first step in image analysis was identification of well-defined labeled endocytic vesicles in the (pH-independent) rhodamine image. Pixels with highest values (excluding the border region) were displayed, five at a time, until most of the endosome centers (generally ~25 in a 4 × 4 μm field) were identified, each consisting of one or more high value pixels. The endosome center, together with one layer of pixels adjacent to the high value pixels, were taken to define the endosome. (Addition of a second layer of pixels generally changed the integrated pixel intensity by <3%). Generally an endosome was defined by 9–20 pixels. A local background intensity for each endosome was determined as the median intensity of the set of pixels located one layer away from the edge of the endosome. The integrated endosome intensity was determined from the summed intensity values of pixels within the endosome border, minus the local background intensity per pixel. Additional endosomes could be added at any time by visually identifying new centers in the image; software-identified objects that were visually judged not to be endosomes, or to be clusters of labeled vesicles, could be deleted. To minimize bias in the selection of additional endosomes, the image was masked by a transfer function so that 30–40 labeled vesicles (defined by a pixel intensity threshold, generally 50–75% of maximum pixel intensity) would appear equally bright.

The x,y locations of endosomes identified in the rhodamine image were sometimes displaced (generally by <2 pixels) in the FITC image because of very small movements of the perfusion chamber/microscope stage, movements of individual endosomes, and/or optical refraction due to the difference in FITC and rhodamine wavelengths. Endosome pixels in the second (FITC) image were identified by first overlaying (in color) the border of endosomes identified in the rhodamine image over the (black and white) FITC image. The FITC image was then shifted (in x and y directions) until the images superimposed. In addition, the borders of each endosome could be shifted individually to optimize alignment using a 2-parameter (x and y displacements) fitting routine in which integrated pixel intensity was maximized. The integrated (background-subtracted) intensity ratios (FITC-to-rhodamine) for all individual endosomes were determined. For determination of endosomal pH, the fluorescence ratio vs. pH data (see Fig. 2 *B*) were fitted to a cubic polynomial; endosomal pH values were calculated by a 2-point calibration procedure in which the cubic polynomial was scaled and offsetted using fluorescence ratios measured at the end of each experiment when cells were exposed to buffers containing high K and nigericin at pH 4 and 8. Pairs of scaling and offset factors were determined in every experiment. Software was written to combine data sets from different cells, display histograms of number of endosomes vs. intensity or pH, and correlate pH with integrated pixel intensities. Data in Figs. 4–7 are the average (weighted by rhodamine intensities) pH for five or more sets of measurements performed on separate cells; 10–25 endosomes were counted and analyzed in each cell. Error bars are the standard deviation of the average pH values from individual cell measurements.

Results

Fig. 1 shows fluorescence micrographs of endocytic vesicles that were pulse labeled for 30 s at 37°C with CF-TMR-Tf (*A*) or CF-TMR-α_2M (*B*). The CF-TMR-Tf–labeled structures were small and distributed throughout the cell cytoplasm; qualitatively, this distribution changed little over 60 min, however the number of labeled vesicles decreased. Further, there was little effect on the distribution of labeled vesicles with anion substitution, or addition of ouabain or the protein kinase activators (see below). The structures labeled by CF-TMR-α_2M or CF-TMR-dextran had a similar appearance for the first 1–3 min, however at later times, they became larger, brighter, and fewer in number, and progressively moved near the cell nucleus as shown for CF-TMR-α_2M in Fig. 1 *B*. These results support the conclusions that Tf is localized in early and recycling endocytic vesicles, whereas α_2M and dextran are routed to late endosomes and lysosomes. Addition of a 50-fold excess of non-fluorescent Tf or α_2M gave a >95% decrease in the number of fluorescent vesicles and in the background-subtracted integrated cellular fluorescence. Setting the temperature to 4°C at the time of labeling with the fluorescent markers also inhibited the integrated cellular fluorescence by >95%. These results indicate that the double-labeled fluorescent Tf and α_2M labels receptor-mediated endosomes, and the fluorescent dextran labels fluid-phase (constitutive) endosomes.

Fig. 1 *C* shows CF-TMF-Tf–labeled endocytic vesicles at a higher magnification. Individual endocytic vesicles are well demarcated as small bright spots. Because the actual diameters of these vesicles is <250 nm, the spots appear as Airy disks (diffraction limited by microscope optics; Inoue, 1989). For the calculation of integrated pixel intensity as described in Materials and Methods, the endocytic vesicles were identified and the boundaries were defined as shown for the image acquired with the rhodamine filter set. The local background intensity, determined from the pixel intensities in an area adjacent to each endosome, consists in principle of fluorescence arising from cytoplasmic dye, and out-of-focus fluorescence from dye bound to the plasma membrane surface and entrapped in other endocytic vesicles. Because the indicators are membrane impermeable, it was predicted that little fluorescence was contributed by cytoplasmic dye; this prediction was confirmed directly by a fluorescence recovery after photobleaching experiment in which a 1-μ spot (in cells viewed 30 min after pulse labeling) was photobleached by an intense laser spot of 2-ms duration (Kao et al., 1992). Fluorescence in the bleached area decreased by 40–50%, but did not recover over time, indicating that there was no dye in the cytoplasmic compartment. In contrast, there was >90% recovery in cells microinjected with the CF-TMR-dextran (recovery half-time ~200 ms). Further, because the fibroblasts are relatively flat, there should be little contribution from out-of-focus endosomes; therefore, the main contribution to the background signal is probably surface dye, with small signals from cell and instrument autofluorescence. The local background subtraction method effectively removed these signal contributions.

The accuracy of our method for determination of pH in individual endocytic vesicles was evaluated from the distribution of fluorescence ratios measured under conditions where all endocytic vesicles should have nearly identical pH. Fig.

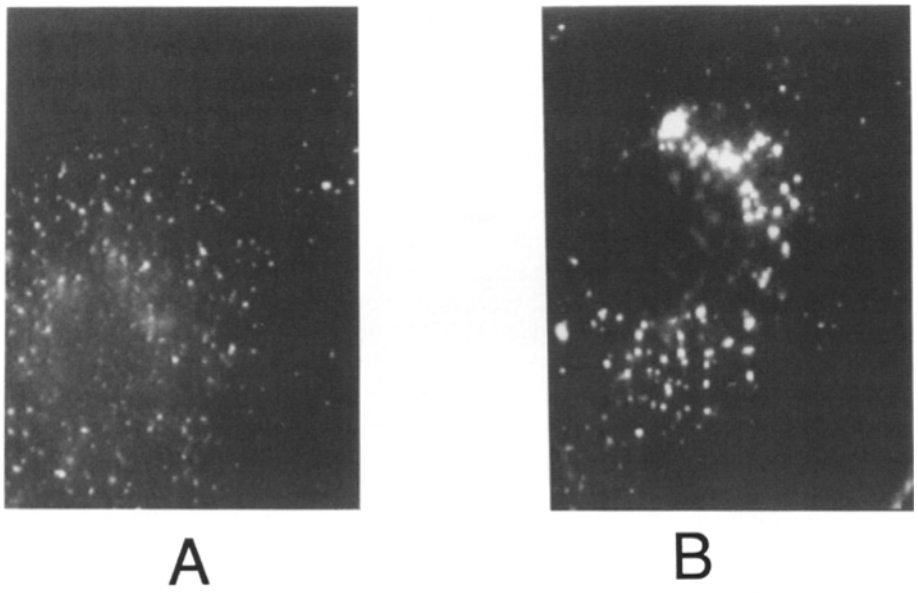

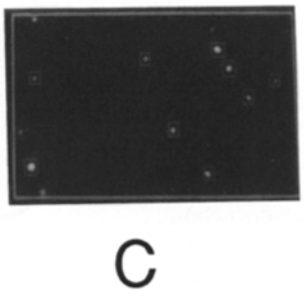

Figure 1. Fluorescence micrographs of fluorescently labeled endocytic vesicles in Swiss 3T3 fibroblasts. Endocytic vesicles were pulsed labeled for 30 s at 37°C with CF-TMR-Tf (*A* and *C*) and CF-TMR-α_2M (*B*). Cells were viewed at 5 min (*A* and *C*) and 20 min (*B*) after labeling. Endosome boundaries are shown in *C* (see text). Final magnifications are 2,100× (*A* and *B*) and 2,700× (*C*).

2 *A* shows a histogram of the number of CF-TMR-Tf labeled endocytic vesicles with specified CF-to-TMR fluorescence ratios. The extracellular solution contained high K and nigericin (at specified pH values) to equilibrate endosomal and extracellular pH. Equilibrium pH was achieved in <2 min as shown by the lack of change in pH upon further incubation for >10 min. The data show a well demarcated distribution of fluorescence ratios, with an SD of ~0.3 ratio units, much smaller than the ~1.2 U difference in ratio per pH unit in the range pH 6–8. Similar results were obtained using CF-TMR-α_2M and CF-TMR-dextran. These results indicate that pH in individual endocytic vesicles can be measured to better than 0.2 pH unit accuracy with these indicators in the pH range 6–8. The pH is less well determined in the range 4–6 (SD = 0.2–0.4 pH unit) because of the decreased sensitivity of the fluorescence ratio to pH. Note that these results represent worst case estimates for the accuracy in pH determination because there is a finite distribution in pH values in individual endosomes, even in the presence of high K and nigericin.

Fig. 2 *B* shows a calibration plot of the averaged fluorescence ratios vs. extracellular pH in solutions containing high K and nigericin. CF-TMR-Tf had an apparent pKa of 6.4 with maximum sensitivity in the pH range 5.5–7. The Cl_2CF-TMR–conjugated indicator had a left-shifted calibration curve with greater pH sensitivity in the range 4–5.5 (pKa 4.9), making it useful for the measurement of pH in very acidic late endosomal and lysosomal compartments. The fluorescence of the CF and Cl_2CF chromophores increased with pH, whereas that of the TMR chromophore was pH independent. The pKa's measured in the endosomes were similar to those of 6.3 (CF-dextran) and 4.8 (Cl_2CF-dextran) measured in cell-free aqueous buffers.

There are several special concerns in the use of an indicator containing different chromophores. The first is differential photobleaching. Since fluorescein bleaches faster than tetramethylrhodamine, photobleaching would cause a drop in fluorescence ratio and in apparent pH. In the measurements reported here, a low incident intensity was selected to avoid photobleaching of either chromophore. The lack of photobleaching was confirmed by demonstrating constant CF and TMR signals in 10 pH measurements obtained 1-min apart for cells bathed in the high K/nigericin buffer (to clamp endosome pH). There was <5% photobleaching of CF when

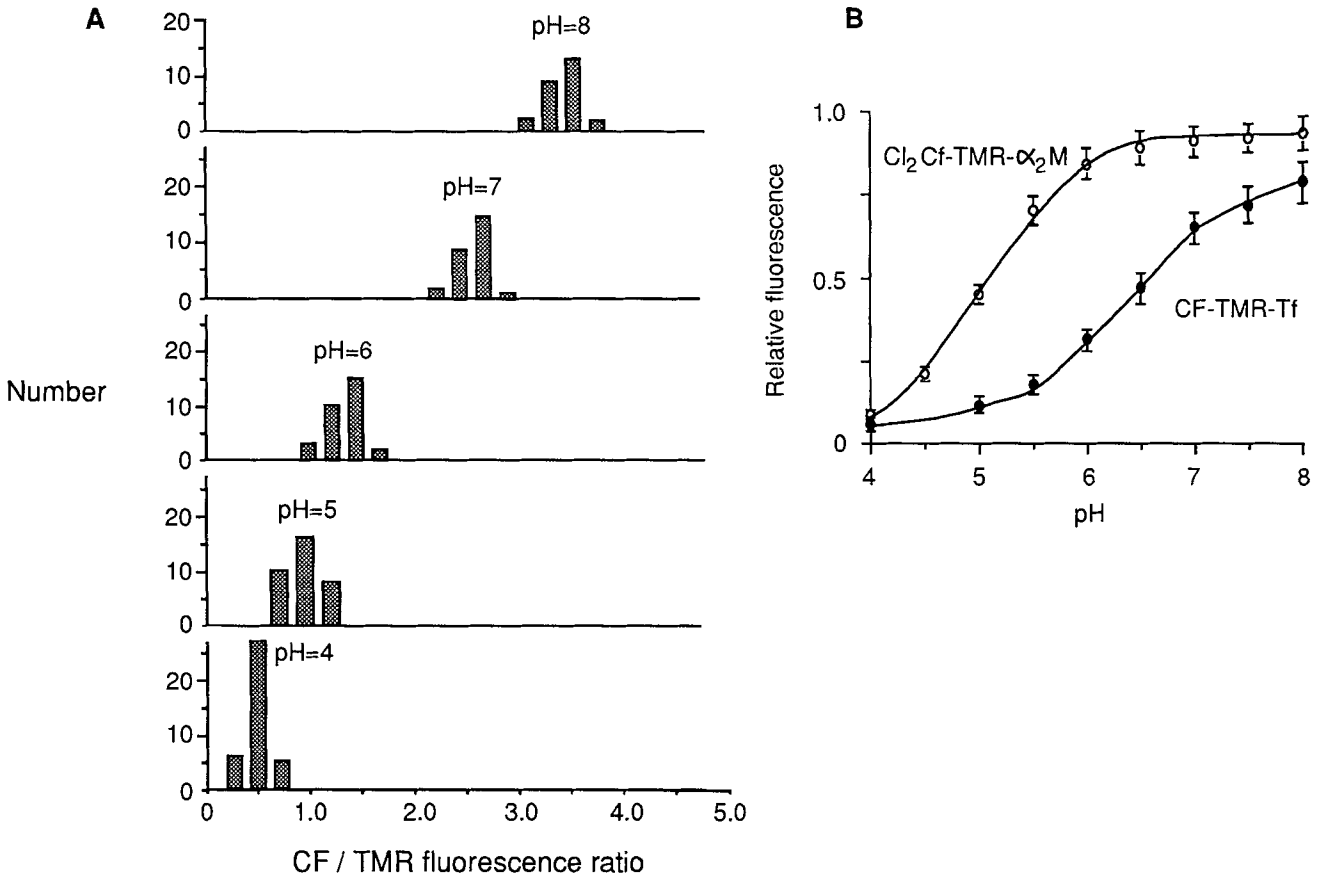

Figure 2. Dependence of fluorescence ratios on pH in labeled endocytic vesicles. (*A*) Endosomes were pulse labeled with CF-TMR-Tf and perfused for 2 min with high K buffers (buffer A with 100 mM Na replaced by K) containing 5 μM nigericin to equilibrate endosomal and extracellular pH. Histograms of the number of endocytic vesicles having specified fluorescence ratios are shown for experiments performed on five separate cells. (*B*) Average CF-to-TMR fluorescence ratios for endocytic vesicles labeled with either CF-TMR-Tf or Cl_2CF-TMR-α_2M.

cells were illuminated continuously for 2 min at the incident intensities used here. The second concern is differential sorting of indicators due to heterogeneous labeling with chromophores; the fluorescence ratio could not be used to calculate pH if indicator molecules with high CF-to-TMR labeling stoichiometry sort into a different compartment than molecules with low labeling stoichiometries. However, there should be little heterogeneity in labeling for the indicators used here in which there were an average of 15 CF and 8 TMR chromophores per Tf, 110 CF or Cl_2CF and 30 TMR chomophores per α_2M, and 8 CF and 4 TMR chromophores per dextran. Further, analysis of the data in Fig. 2 *A* showed no correlation between the position of labeled vesicles in the distributions obtained at different pH. Similar results were obtained for the CF-TMR-α_2M and CF-TMR-dextran. These results indicate that differential sorting of labeled indicators does not occur in these experiments. A third concern is that endosome movement during the measurement might give an incorrect fluorescence ratio. This possibility is unlikely because the rhodamine and FITC images were acquired rapidly (generally <3 s total acquisition time for image pair), vesicle movement is slow, and the integrated pixel intensity is relatively insensitive to the exact focus position. Experimentally, for studies of CF-TMR-Tf and CF-TMR-α_2M trafficking as described below, pH values did not depend on the order of the rhodamine and FITC image acquisitions.

The pH distributions in a cohort of endocytic vesicles at various times after pulse labeling with CF-TMR-Tf and (CF-TMR-α_2M or Cl_2CF-TMR-α_2M) are shown in Fig. 3. For endosomes labeled with CF-TMR-Tf, there is a progressive decrease in the median pH of the distribution over the first 10 min to a minimum average pH of ~6.2. Very few endocytic vesicles had a pH <6.0 at any time. Interestingly, the average pH increased slightly from 10 to 15 min after labeling, consistent with the trafficking of Tf-labeled vesicles from early to recycling endosomes (Sipe and Murphy, 1987; Yamashiro and Maxfield, 1987*a*). In contrast, endocytic vesicles labeled with the fluorescent α_2M strongly acidified over time to pH <5. To maximize the sensitivity of the pH measurements, data for the first 10 min are shown for CF-TMF-α_2M, and for >10 min for Cl_2CF-TMR-α_2M. The average pH of late endosomes/lysosomes was 4.7. Interestingly, a small fraction of endocytic vesicles strongly acidified in the first min after labeling. From eight sets of experiments performed with CF-TMR-α_2M or Cl_2CF-α_2M as fluorescent labels, ~15% of endosomes had pH <5.5 at 1 min. For comparison, no endosome labeled with Tf had pH <5.5 at any time. Note that the 15% estimate must be considered approximate because of the finite width of the distributions given

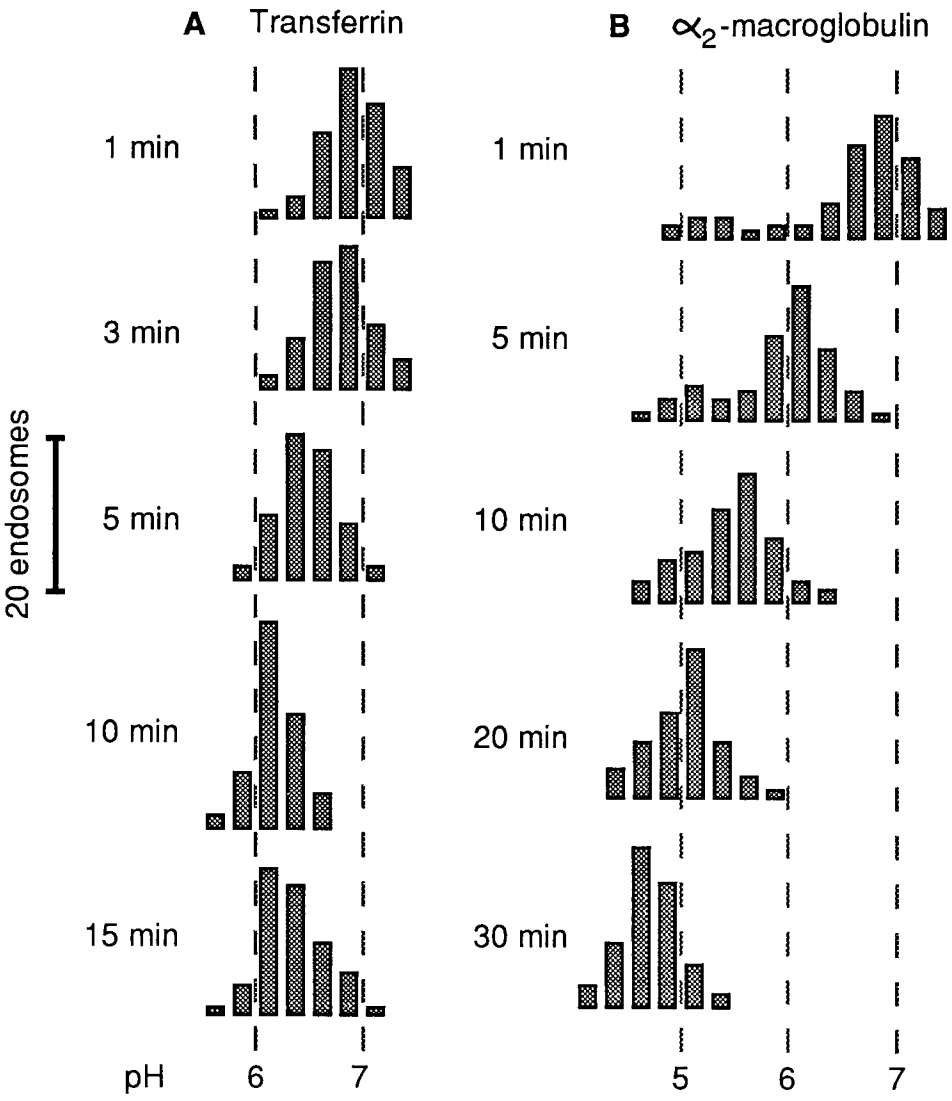

Figure 3. Time course of pH distributions in endocytic vesicles labeled with Tf (*A*) and α_2M (*B*). Endocytic vesicles were pulse labeled for 30 s and the time course of pH was measured at 37°C using a physiological solution containing chloride (buffer A). The pH of individual endocytic vesicles was measured in five separate experiments. Histograms were generated by counting endosomes in 0.25 unit pH intervals. For the α_2M data, pH distributions for time >10 min were taken from vesicles labeled with Cl_2CF-TMR-α_2M.

in Fig. 2 *A*. Further, although we were careful to avoid the selection of brighter labeled vesicles (see Materials and Methods), it is possible that the late endosomes might be overrepresented because of their increased size and brightness.

The pH values (mean and SD) for endocytic vesicles labeled with fluorescent Tf, α_2M, and dextran are given in Fig. 4. Tf-labeled endocytic vesicles acidified to pH 6–6.2 with a half-time of ~4 min (*A*), whereas α_2M (*B*), and dextran-labeled (*C*) endosomes progressively acidified to pH ~5 over >20 min. Fig. 4 also shows the effect of replacement of extracellular chloride by the cell-permeant anion NO_3, or the cell-impermeant anion isethionate. In these studies, cells were first pulse labeled with the fluorescent indicator in the presence of extracellular Cl (solution A) because endocytic uptake was strongly inhibited upon replacement of Cl by NO_3 or isethionate. After labeling at 37°C, cells were cooled immediately by perfusion with buffers B (containing NO_3) or C (containing isethionate) for 10 min at 10°C. The incubation at low temperature effectively inhibited endocytic trafficking, but allowed the efflux of intracellular Cl to occur; intracellular Cl activity was <10 mM at the completion of the low temperature incubation as assessed by the SPQ fluorescence method (Chao et al., 1989). Fig. 4 (*A–C*) shows that replacement of Cl by NO_3 or isethionate strongly inhibited acidification of endosomes containing either receptor-mediated or fluid-phase probes. Fig. 4, *D* and *E* show that addition of Cl after partial acidification reversed the inhibitory effect, resulting in prompt acidification to values near those obtained in the uninterrupted presence of Cl. Fig. 4 *F* shows that removal of Cl after acidification caused alkalinization, indicating that the acidification was reversible.

The effects of inhibition of the Na/K ATPase by ouabain on endosomal acidification were next examined. Cells were incubated with 0 mM (−ouabain) or 1 mM (+ouabain) ouabain for 5 min before and during the labeling period to facilitate ouabain binding to plasma membrane Na/K ATPase. Ouabain was then removed from the extracellular buffer for all subsequent pH measurements in Fig. 5, *A* and *B*. There was a large effect of ouabain on endosomal acidification at early times. Fig. 5 *A* shows that ouabain increased acidification by ~0.8 pH units at 1 min after labeling. Although there was no change in the morphology of the Tf-labeled endocytic vesicles, ouabain decreased the minimum pH to ~5.3, much

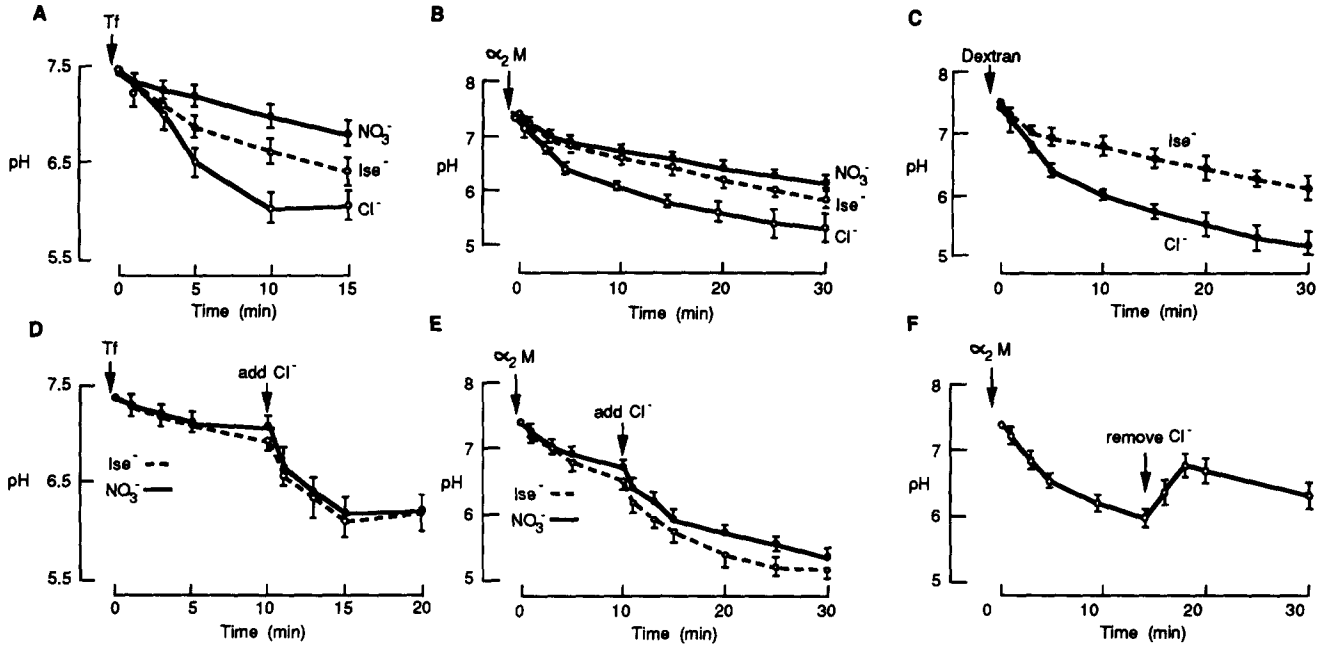

Figure 4. Effect of anion substitution on endosomal acidification. Endosomes were labeled with CF-TMR-Tf, CF-TMR-α_2M, or CF-TMR dextran for 30 s at 37°C. Cells were then perfused with buffers A, B, or C for 10 min at 10°C to allow for anion equilibration without endosomal trafficking. Cells were then perfused with the corresponding buffers at 37°C for determination of the time course of pH. Data are the mean and SD for measurements in five separate cells (see Materials and Methods). In *D* and *E*, buffers B or C were replaced with buffer A (containing Cl) where indicated. In *F*, buffer A was replaced by buffer C (containing isethionate).

less than that of ~6.2 in the absence of ouabain, and nearly as low as the pH of very late endosomes and lysosomes. In the α_2M-labeled endocytic vesicles (Fig. 5 *B*), ouabain strongly enhanced acidification over the first 20 min, although the minimum pH obtained in late endosomes and lysosomes was independent of ouabain. Similar results were obtained for dextran-labeled endocytic vesicles (not shown).

Further experiments were carried out to investigate whether the effect of ouabain was at plasma or endosomal membrane sites. Fig. 5 *C* shows no effect of addition of extracellular ouabain to cells that had been labeled in the absence of ouabain (compare with Fig. 5 *A*, "−ouabain" data). Similarly, addition of extracellular ouabain had no effect on endosomal acidification in cells that had been labeled in the presence of ouabain (not shown). These results provide evidence that the site of action of ouabain is within endosomal vesicles. The Na/K ATPase (with bound ouabain) is presumably internalized at the time of endocytosis. Fig. 5 *D* shows that the presence of ouabain at the time of labeling enhanced acidification even when Cl was replaced by isethionate. Addition of Cl at 15 min after labeling then gave maximum acidification to values similar to those obtained in the uninterrupted presence of Cl. These results suggest that both the presence of Cl and the activity of the Na/K ATPase affects endosomal acidification (see Discussion).

The effect of protein kinase A activation by cAMP agonists was next examined. In Fig. 6 *A*, cells were incubated with 0 or 0.5 mM chlorophenylthio-cAMP (CPT-cAMP) for 10 min before, and then during and after the pulse labeling with CF-TMR-Tf. CPT-cAMP inhibited endosomal acidification significantly; removal of CPT-cAMP at 10 min reversed the inhibitory effect. Fig. 6 *B* shows that addition of CPT-cAMP or forskolin at a time when nearly complete endosomal acidification occurred caused an increase in pH. Fig. 6 *C* shows a slight inhibition of early endosomal acidification in CF-TMR-α_2M–labeled endocytic vesicles. There was no significant effect of CPT-cAMP on the maximum acidification in late endosomes and lysosomes observed at >20 min after labeling. Fig. 6 *D* shows the combined effects of CPT-cAMP and ouabain on endosomal acidification. 1 mM ouabain was present for 5 min before and during the pulse labeling with CF-TMR-Tf; 0.5 mM CPT-cAMP was present throughout. The curve labeled "-CPT-cAMP," shown for comparison, is the same as in Fig. 5 *A* ("+ouabain" curve). The data show that CPT-cAMP is effective even when the Na/K ATPase is inhibited, indicating that CPT-cAMP does not inhibit acidification by stimulation of Na/K ATPase pump activity.

The effects of activation of phospholipase C on endosomal acidification were examined in Fig. 7. Fig. 7 *A* shows that cells preincubated with 50 nM vasopressin, and perfused continuously with vasopressin during and after labeling, had a small but significantly enhanced endosomal acidification compared to control cells. The enhanced acidification was also observed upon addition of vasopressin at 5 min after pulse labeling (Fig. 7 *B*). Note that the dashed curve in Fig. 7 *B* shown for comparison is the same as the dashed curve in Fig. 7 *A*. The activation of phospholipase C by vasopressin binding to V1 receptors gives a transient elevation of intracellular Ca and rapid activation of protein kinase C (Issandou and Rozengurt, 1990). These factors were investigated independently. The continued and strong elevation of intracellular Ca by the ionophore A23187 had no significant effect on endosomal acidification (Fig. 7 *C*), whereas activation of protein kinase C by PMA strongly enhanced endosomal acidification in the Tf-labeled endosomes (Fig. 7 *D*). Cells

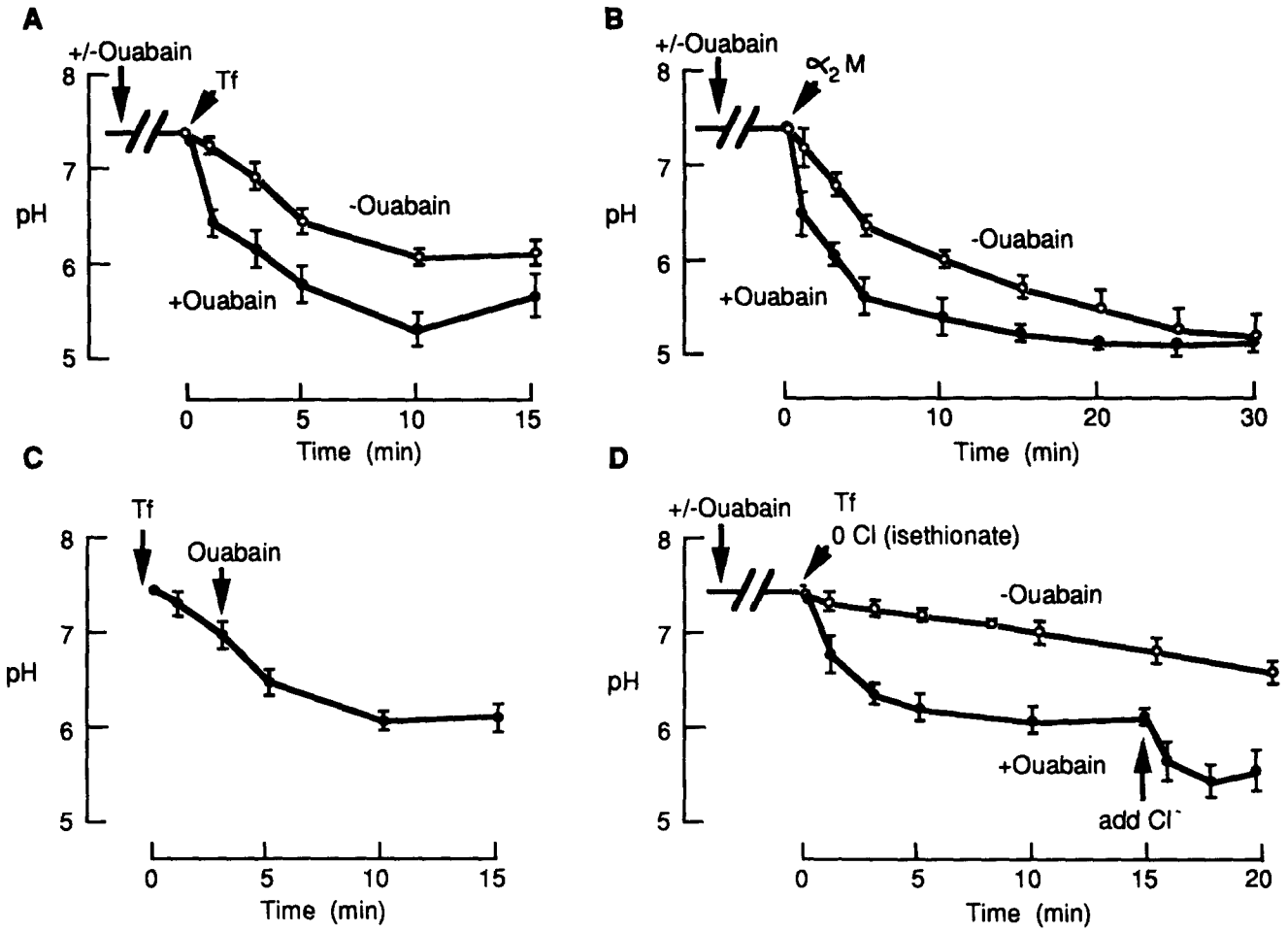

Figure 5. Effect of inhibition of the Na/K ATPase by ouabain on endosomal acidification. (*A* and *B*) Where indicated, cells were incubated for 5 min with 0 or 1 mM ouabain before labeling and during the 30-s pulse labeling with CF-TMR-Tf or CF-TMR-α_2M. Cells were then perfused with buffer A (containing Cl) at 37°C in the absence of ouabain for measurement of the time course of pH. (*C*) Ouabain was added to the extracellular solution where indicated to cells that were labeled in the absence of ouabain. (*D*) Cells were incubated for 5 min in buffer A containing 0 or 1 mM ouabain and labeled for 30 s with CF-TMR-Tf in buffer A. Cells were then incubated for 10 min at 10°C in buffers A (Cl) or C (isethionate). Where indicated buffer C was switched back to buffer A.

preincubated for 10 min with PMA and studied in the continued presence of PMA showed a rapid acidification to a minimum pH of ~5.7. In cells that had not been exposed to PMA, the addition of PMA at 5 min after endosome labeling gave a similar enhancement of acidification.

Discussion

The goals of this study were (*a*) To measure pH accurately in the range 4–8 in individual fluorescently labeled endocytic vesicles in viable fibroblasts; and (*b*) to determine whether acidification was regulated by intracellular Cl, Na/K pump inhibition, and intracellular second messengers. The rationale for studies of intracellular Cl and cAMP effects was the observations in cell-free systems that the limiting membranes of endocytic compartments generally contain Cl channels (Van Dyke, 1988; Barasch et al., 1988; Blair et al., 1991), which in some systems, are activated by protein kinase A–dependent phosphorylation (Bae and Verkman, 1990; Mulberg et al., 1991). The rationale for studies of Na/K pump inhibition was the observation that incubation of A549 cells with ouabain-enhanced acidification in transferrin-labeled endosomes (Cain et al., 1989; Fuchs et al., 1989*b*). Direct and phospholipase C–mediated protein kinase C activation was studied because of the diverse effects of phorbol esters on intracellular trafficking in multiple cell types (Backer and King, 1991). The purpose of the measurements reported here was to survey and characterize the effects of purported modulators of endosomal acidification in fibroblasts. The definition of detailed regulatory mechanisms will require evaluation of electrochemical driving forces in cell-free systems and intact cells, involving challenging measurements of endosomal electrical potentials, and endosomal and cytoplasmic ion activities.

The methodology developed here to measure pH in individual endocytic vesicles is an extension of imaging methods reported for cell-free studies of heterogeneity in ATP-dependent acidification in isolated endosomes from kidney cortex (Shi et al., 1991). Compared to whole-cell estimates of endosomal pH by cell sorting or cell-integrated imaging, mea-

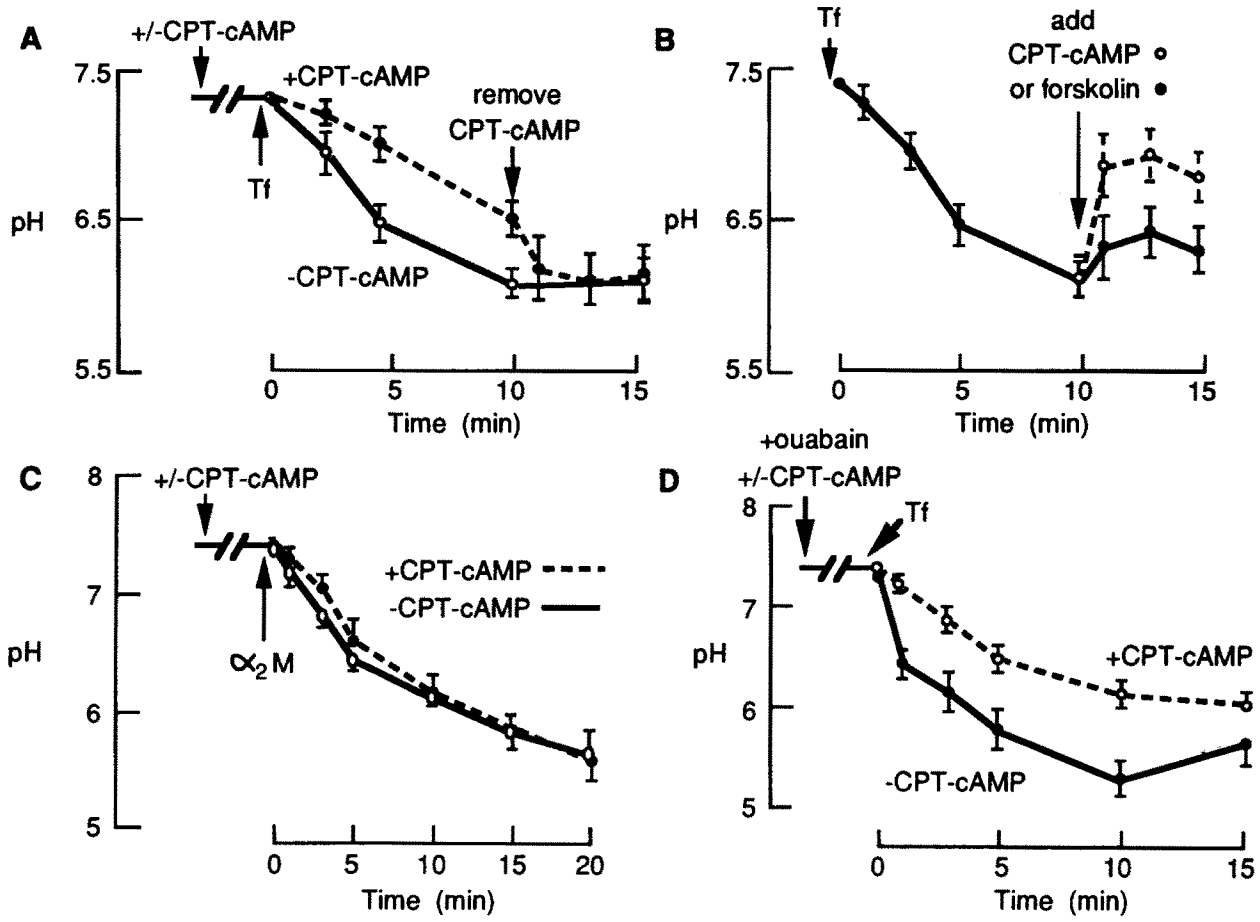

Figure 6. Effects of protein kinase A activation on endosomal acidification. All measurements were performed with buffer A. (*A* and *C*) Cells were perfused with 0 or 0.5 mM CPT-cAMP for 5 min before, during, and after labeling with CF-TMR-Tf (*A*) or CF-TMR-α_2M (*C*). CPT-cAMP was removed from the extracellular solution where indicated. (*B*) 0.5 mM CPT-cAMP or 10 μM forskolin were added 10 min after pulse labeling with CF-TMR-Tf. (*D*) Cells were perfused with 0 or 0.5 mM CPT-cAMP before, during, and after labeling with CF-TMR-Tf. 1 mM ouabain was present for 5 min before and during labeling.

surements on individual vesicles have several advantages: (*a*) The (number vs. pH) distribution of pH values can be determined, providing information about heterogeneous intracellular processes; (*b*) contributions to the fluorescence signal from dye bound to the external surface are removed effectively; and (*c*) endosomal pH can be correlated with morphology. The potential difficulties in the measurement of pH in individual endocytic compartments are the weak signal from fluorescently labeled vesicles as small as 100-nm diam, photobleaching effects, time-dependent changes in morphology, out-of-focus signal from surface and cytoplasmic dye, out-of-focus signal from dye in other endosomes, and possible differences in fluorescence vs. pH calibrations in different endocytic compartments (Maxfield and Dunn, 1989). Another concern is that some vesicles with low fluorescence might be missed, potentially skewing the analysis to exclude a selected subpopulation of endosomes. Finally, the fluorescent label must remain chemically intact and provide relatively large changes in signal with pH to overcome the signal-to-noise limitations in single vesicle measurements.

Our approach to measure pH in individual endocytic vesicles involved quantitative ratio imaging of fluorescently labeled vesicles in adherent cells. Endocytic vesicles were pulse labeled with fluorescent probes in situ in a perfusion chamber in which solutions were exchanged continuously and effectors could be added and removed at specified times. The synthesized fluorescent labels of receptor-mediated and fluid-phase endocytosis were chosen to give strong signals with little photobleaching. Both pH-sensitive and -insensitive chromophores (Cain and Murphy, 1988) were conjugated to each protein or dextran molecule (rather than making use of the intrinsic pH dependence of the FITC excitation spectrum) to maximize the sensitivity of the fluorescence ratio to pH; in addition, because carboxyfluorescein (and FITC) fluorescence is relatively insensitive to pH in the range 4.5–5.5, a dichlorocarboxyfluorescein-tetramethylrhodamine conjugate was used to measure pH accurately in the very acidic late endocytic and lysosomal compartments. An important component of the measurement process was the sensitive imaging hardware, consisting of a 1.4 NA objective, electronic shutters to minimize light exposure, and a cooled CCD camera with a very sensitive detector having a quantum efficiency of >0.85 at wavelengths used in this study. Further, the specialized software routines, as described in the Materials and Methods section, made possible the identification of endosomes, the subtraction of background, and

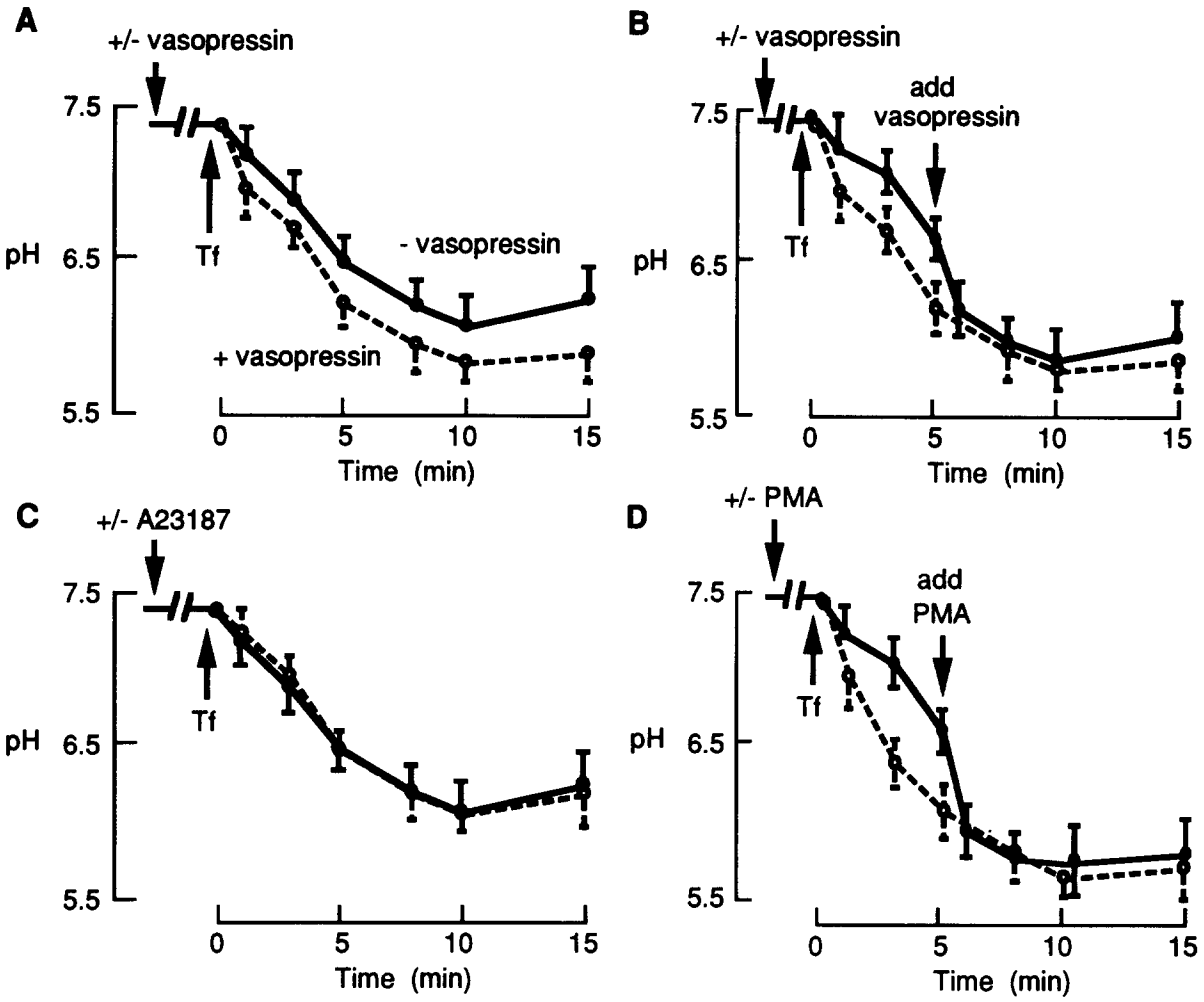

Figure 7. Effects of phospholipase C, Ca, and protein kinase C activation on endosomal acidification. All measurements were performed with buffer A. (*A* and *B*) Cells were perfused with 0 or 50 nM vasopressin for 10 min before, during, and after labeling with CF-TMR-Tf. Where indicated in *B*, vasopressin was added 5 min after labeling. (*C*) Cells were perfused for 10 min before, during, and after labeling with buffer A containing 0 (—) or 1 μM (---) A23187. (*D*) Cells were perfused for 10 min before, during, and after labeling with 0 (—) or 100 nM (---) PMA. Where indicated, PMA was added to the extracellular buffer at 5 min after perfusion in the absence of PMA.

the calculation of intensity ratios of integrated single endosome signals. Although experiments were carried out on a Nipkow wheel coaxial-confocal microscope with selectable pinhole size, quantitative measurements were carried out in the wide-field mode because the cells were relatively flat, the signal intensities were higher, and most importantly, the narrow point-spread-function of confocal optics makes difficult the quantitative determination of endosome-integrated signals without obtaining images at multiple z-planes. A confocal approach has been applied to studies of endosome fusion in intact cells (Benveniste et al., 1989), and may be required for quantitative measurements of endosomal acidification in cells having greater z-thickness. The accuracy of pH measurements in individual endocytic vesicles was validated in calibration studies in which endosomal and extracellular pH were equalized by high K and the ionophore nigericin. Our general approach to measure pH in individual endosomes was similar to that developed by Maxfield and colleagues in a series of elegant papers (Dunn et al., 1989; Yamashiro et al., 1987*a*,*b*, 1989), however there are notable differences that we believe to be important in the fluorescent markers, imaging hardware, and analysis routines.

It is established that transferrin and its receptor are routed through early endosomes to recycling endosomes that are destined to fuse with the plasma membrane (Dautry-Varsat et al., 1983). In our experiments, transferrin-labeled endosomes were visible as small dots distributed throughout the cell. No uptake was observed in the presence of an excess of non-fluorescent transferrin, indicating uptake only by receptor-mediated endocytosis. The morphology of the fluorescent transferrin-labeled endosomes did not change remarkably over time, or with the various regulatory compounds tested. Inhibition of the Na/K pump by ouabain strongly enhanced the initial rate of acidification and the maximum acidification of the transferrin-labeled endosomes. The enhanced acidification required the presence of ouabain at the time of fluorescence labeling; the presence of extracellular ouabain after labeling had no effect on endosomal acidification. These findings support the conclusions of Fuchs et al. (1989) and Cain et al. (1989) that

acidification to pH <6 in early and recycling endosomes is prevented by a functional Na/K ATPase on the endosomal membrane, which presumably is present because of endocytic retrieval of plasma membrane Na/K pumps. Our data further indicate that an Na/K ATPase strongly modulates early acidification not only in receptor-mediated endocytosis of transferrin, but also in receptor-mediated endocytosis of α_2-macroglobulin, a ligand routed to lysosomes (Yamashiro et al., 1989), and the fluid-phase endocytosis of dextran. The regulation of pH in early endosomes by an Na/K ATPase is probably not a general feature in all cell types. Sipe et al. (1991) showed that transferrin-labeled endosomes acidified to pH <5.5 in erythroleukemia cells; similarly, it is unlikely that acidification in apical membrane endosomes in epithelial cells is regulated by an Na/K ATPase because the Na/K ATPase is a basolateral, rather than an apical or endosomal membrane component (Hilden et al., 1990).

Activation of protein kinase C by PMA also strongly enhanced early acidification in receptor-mediated endosomes. Similar, though less pronounced acidification was observed by receptor-mediated activation of phospholipase C by vasopressin, giving both protein kinase C activation and an elevation in intracellular ionized Ca. Elevation of Ca alone by ionophores did not affect endosomal acidification. The mechanism by which protein kinase C enhanced acidification cannot be determined from these studies. Although effects on endosomal acidification have not been reported, activation of protein kinase C has been demonstrated to have multiple effects on receptor-mediated endocytosis (for review see Backer and King, 1991), including ligand-independent down-regulation of the transferrin receptor, serine and tyrosine phosphorylation of various receptors, and other heterogeneous effects on receptor trafficking. Activation of protein kinase C also probably causes a non-specific increase in fluid-phase endocytosis in epithelial cells (Shi et al., 1990). The physiological role of the protein kinase C-enhanced endosomal acidification is unknown.

The replacement of extracellular Cl by NO_3 or isethionate strongly inhibited endosomal acidification. NO_3 is cell permeable and has been reported to inhibit the vacuolar-type proton pump directly (Van Dyke, 1986). Isethionate is relatively cell impermeable and is unlikely to act by direct proton pump inhibition. The inhibition of endosomal acidification in response to replacement of Cl by isethionate is consistent with a requirement for intracellular Cl to shunt the interior positive potential produced by the proton pump (Barasch et al., 1988), and/or for allosteric activation of the proton pump (Moriyama and Nelson, 1987). Note that both the endosomal Cl conductance and Na/K pump activity can control acidification independently (potentially in synergy) because their regulatory mechanisms are different. Whereas the Na/K pump produces an interior-positive membrane potential to oppose proton pumping, the Cl conductance provides the counterion to maintain electroneutrality. The observation that protein kinase A activation by forskolin or a cell-permeable cAMP analog inhibited endosomal acidification suggests that activation of an endosomal Cl channel in fibroblasts does not occur, or is of minor importance compared to other cAMP-dependent regulatory mechanisms.

The acidification data obtained here cannot be used to define convincingly the transporter(s) and/or pump(s) that are influenced by anion substitution and protein kinase activation. Further, it is possible that some of the agonists alter the rates of endosomal trafficking and thus acidification in a secondary manner. However, the reversibility of the effects of anion substitution and protein kinase A activation are not consistent with a direct influence on trafficking. (It is unlikely that an endocytic marker would move from a later to an earlier compartment.) Further, the characteristic appearance of the early Tf-labeled endosomes was not influenced by ouabain, anion substitution and protein kinase activation, suggesting that the increased acidification associated with these maneuvers was not associated with a major difference in endosome stage, although it is not correct to infer precise information about endosome stage by appearance alone. Further analysis of agonist effects on endosome trafficking will require morphological identification of labeled compartments in intact cells, and membrane transport studies in cell-free preparations.

The pH of very late endosomes (probably lysosomes) was determined to be 4.7 $\pm$ 0.2. Whereas acidification in early endosomes was subject to regulation by multiple factors, lysosomal pH was not sensitive to Na/K pump inhibition or protein kinase activation. These results are consistent with the relatively large conductances to anions and cations in lysosomes (Forster and Lloyd, 1988). Further, the lack of effect of ouabain and activation of protein kinases on lysosome pH suggests that the effects of these agents on acidification in early endosomes is not due to a direct modulation of the vacuolar proton pump. Another interesting finding was that a small portion of internalized α_2-macroglobulin was routed rapidly to lysosomes so that ~15% of labeled vesicles had a pH of <5.5 at 1 min after labeling. Examination of the time course of the distribution of pH values (Fig. 3) raises the possibility that there may exist a rapid route for lysosomal trafficking of a subpopulation of internalized ligands. Further studies involving single endosome tracking will be required to elucidate the nature of such a specialized pathway.

This work was supported by grants HL42368, DK39354, DK43840, and DK35124 from the National Institutes of Health and a grant from the Cystic Fibrosis Foundation. Dr. Biwersi was supported by a fellowship from the National Cystic Fibrosis Foundation. Dr. Verkman is an established investigator of the American Heart Association.

Received for publication 24 March 1992 and in revised form 30 June 1992.

References

Backer, J. M., and G. L. King. 1991. Regulation of receptor-mediated endocytosis by phorbol esters. *Biochem. Pharm.* 41:1267–1277.

Bae, H.-R., and A. S. Verkman. 1990. Protein kinase A regulates chloride conductance in endocytic vesicles from proximal tubule. *Nature (Lond.).* 348:635–637.

Barasch, J., M. D. Gershon, E. A. Nunez, H. Tamir, and Q. Al-Awqati. 1988. Thyrotropin induces the acidification of the secretory granules of parafollicular cells by increasing the chloride conductance of the granular membrane. *J. Cell Biol.* 107:2137–2147.

Barasch, J., B. Kiss, A. Prince, L. Saiman, D. Gruenert, and Q. Al-Awqati. 1991. Defective acidification of intracellular organelles in cystic fibrosis. *Nature (Lond.).* 352:70–73.

Benveniste, M., J. Schlessinger, and Z. Kam. 1989. Characterization of internalization and endosome formation of epidermal growth factor in transfected NIH-3T3 cells by computerized image-intensified three-dimensional fluorescence microscopy. *J. Cell Biol.* 109:2105–2115.

Blair, H. C., S. L. Teitelbaum, H.-L. Tan, C. M. Koziol, and P. H. Schlesinger. 1991. Passive Cl permeability charge coupled to H^+ATPase of avian osteoclast ruffled membrane. *Am. J. Physiol.* 260:C1315–C1324.

Cain, C. C., and R. F. Murphy. 1988. A chloroquine-resistant Swiss 3T3 cell line with a defect in late endocytic acidification. *J. Cell Biol.* 106:269–277.

Cain, C. C., D. M. Sipe, and R. F. Murphy. 1989. Regulation of endocytic pH by the Na^+, K^+-ATPase in living cells. *Proc. Natl. Acad. Sci. USA.* 86:544–548.

Chao, A. C., J. A. Dix, M. Sellers, and A. S. Verkman. 1989. Fluorescence measurement of chloride transport in monolayer cultured cells: mechanisms of chloride transport in fibroblasts. *Biophys. J.* 56:1071–1081.

Cuppoletti, J., D. Aures-Fischer, and G. Sachs. 1987. The lysosomal H^+ pump: 8-azido ATP inhibition and the role of chloride in H^+ transport. *Biochem. Biophys. Acta.* 899:276–284.

Dautry-Varsat, A., A. Ciechanover, and H. F. Lodish. 1983. pH and the recycling of transferrin during receptor-mediated endocytosis. *Proc. Natl. Acad. Sci. USA.* 80:2258–2262.

Dunn, K. W., T. E. McGraw, and F. R. Maxfield. 1989. Iterative fractionation of recycling receptors from lysosomally destined ligands in an early sorting endosome. *J. Cell Biol.* 109:3303–3314.

Forster, S., and J. B. Lloyd. 1988. Solute translocation across the mammalian lysosome membrane. *Biochim. Biophys. Acta.* 947:465–491.

Fuchs, R., P. Male, and I. Mellman. 1989. Acidification and ion permeabilities of highly purified rat liver endosomes. *J. Biol. Chem.* 264:2212–2220.

Fuchs, R., S. Schmid, and I. Mellman. 1989. A possible role for Na^+, K^+-ATPase in regulating ATP-dependent endosome acidification. *Proc. Natl. Acad. Sci. USA.* 86:539–543.

Gruenberg, J., and K. E. Howell. 1989. Membrane traffic in endocytosis: insights from cell-free assays. *Ann. Rev. Cell Biol.* 5:453–481.

Hilden, S. A., K. B. Ghoshroy, and M. E. Madias. 1990. Na/H exchange, but not Na/K ATPase, is present in endosome-enriched microsomes from rabbit renal cortex. *Am. J. Physiol.* 258:F1311–F1319.

Hopkins, C. R., A. Gibson, M. Shipman, and K. Miller. 1990. Movement of internalized ligand-receptor complexes along a continuous endosomal reticulum. *Nature (Lond.).* 346:335–339.

Inoue, S. 1989. Imaging of unresolved objects, superresolution and precision of distance measurement, with video microscopy. *In* Methods in Cell Biology. Vol. 30. D. L. Taylor and Y.-L. Wang, editors. 85–112.

Issandou, M., and E. Rozengurt. 1990. Bradykinin transiently activates protein kinase C in Swiss 3T3 cells. Distinction from activation by bombesin vasopressin. *J. Biol. Chem.* 265:11890–11896.

Kao, H. P., J. R. Abney, and A. S. Verkman. 1992. Determinants of the mobility of a small solute in the cytoplasm of Swiss 3T3 fibroblasts. *J. Cell Biol.* In review.

Lencer, W. I., A. S. Verkman, D. A. Ausiello, A. Arnaout, and D. Brown. 1990. Endocytic vesicles from renal papilla which retrieve the vasopressin-sensitive water channel do not contain an H^+ ATPase. *J. Cell Biol.* 111: 379–389.

Lukacs, G. L., O. D. Rotstein, and S. Grinstein. 1991. Determinants of the phagosomal pH in macrophages. In situ assessment of vacuolar H^+-ATPase activity, counterion conductance, and H^+ leak. *J. Biol. Chem.* 266:24540–24548.

Maxfield, F. R., and K. W. Dunn. 1989. Studies of endocytosis using image intensification fluorescence microscopy and digital image analysis. *In* Digitized Video Microscopy. B. Herman and K. Jacobson, editors. Alan R. Liss, Inc., New York.

Mellman, I., R. Fuchs, and A. Helenius. 1986. Acidification of the endocytic and exocytic pathways. *Ann. Rev. Biochem.* 55:663–700.

Moriyama, Y., and N. Nelson. 1987. The purified ATPase from chromaffin granule membranes is an anion-dependent proton pump. *J. Biol. Chem.* 262:9175–9180.

Mulberg, A. E., B. M. Tulk, and M. Forgac. 1991. Modulation of coated vesicle chloride channel activity and acidification by reversible protein kinase A-dependent phosphorylation. *J. Biol. Chem.* 266:20590–20593.

Reenstra, W., I. Sabolic, H.-R. Bae, and A. S. Verkman. 1992. Protein kinase A dependent membrane protein phosphorylation and Cl conductance in endosomal vesicles from kidney cortex. *Biochemistry.* 31:175–181.

Sabolic, I., F. Waurin, L. B. Shi, A. S. Verkman, D. A. Ausiello, and D. Brown. 1992. Apical endosomes from collecting duct principal cells lack subunits of the proton pumping ATPase. *J. Cell Biol.* In press.

Shi, L.-B., K. Fushimi, H.-R. Bae, and A. S. Verkman. 1991. Heterogeneity in acidification measured in individual endocytic vesicles isolated from kidney proximal tubule. *Biophys. J.* 59:1208–1217.

Shi, L.-B., Y.-X. Wang, and A. S. Verkman. 1991. Regulation of the formation and water permeability of endosomes from toad bladder granular cells. *J. Gen. Physiol.* 96:789–808.

Sipe, D. M., and R. F. Murphy. 1987. High-resolution kinetics of transferrin acidification in BALB/3T3 cells exposed to pH 6 followed by temperature sensitive alkalinization during recycling. *Proc. Natl. Acad. Sci. USA.* 84:7119–7123.

Sipe, D. M., A. Jesurum, and R. F. Murphy. 1991. Absence of Na^+, K^+-ATPase regulation of endosomal acidification in K562 erythroleukemia cells: analysis via inhibition of transferrin recycling by low temperatures. *J. Biol. Chem.* 226:3469–3474.

Van Dyke, R. W. 1986. Anion inhibition of the proton pump in rat liver multivesicular bodies. *J. Biol. Chem.* 261:15941–15948.

Van Dyke, R. W. 1988. Proton-pump generated electrochemical gradients in rat liver multivesicular bodies. Quantitation and effects of chloride. *J. Biol. Chem.* 263:2601–2611.

Wang, Y.-X., L.-B. Shi, and A. S. Verkman. 1991. Functional water channels and proton pumps are in separate populations of endocytic vesicles from toad bladder granular cells. *Biochemistry.* 30:2888–2894.

Yamashiro, D. J., and F. R. Maxfield. 1984. Acidification of endocytic compartments and the intracellular pathways of ligands and receptors. *J. Cell Biol.* 26:231–246.

Yamashiro, D. J., and F. R. Maxfield. 1987*a*. Kinetics of endosome acidification in mutant and wild-type Chinese hamster ovary cells. *J. Cell Biol.* 105:2713–2721.

Yamashiro, D. J., and F. R. Maxfield. 1987*b*. Acidification of morphologically distinct endosomes in mutant and wild-type Chinese hamster ovary cells. *J. Cell Biol.* 105:2723–2733.

Yamashiro, D. J., L. A. Borden, and F. R. Maxfield. 1989. Kinetics of α_2-macroglobulin endocytosis and degradation in mutant and wild-type Chinese hamster ovary cells. *J. Cell. Physiol.* 139:377–382.